

Low frequency results for the radio galaxies and the role of GMRT

Dharam Vir Lal

MPI für Radioastronomie, Auf dem Hügel 69, 53121 Bonn, Germany.

Abstract. We have studied several radio galaxies at low radio frequencies using GMRT. Our prime motivation to detect faint radio emission at very low frequencies due to low energy electrons.

Our results provide evidence that there exists two classes of sources on morphological grounds. The first class is explained by the simple picture of spectral electron ageing but in the second class the low-frequency synchrotron emission fades (nearly) as rapidly as high-frequency synchrotron emission. In addition, in several sources, the spectra of low-surface-brightness features are flatter than the spectra of high-surface-brightness features, which suggests that either the simple picture of spectral electron ageing needs revision or we need to re-examine the formation mechanism of such sources.

The images and statistics, and the relevance of these results along with the role of GMRT in exploring several unknowns are presented.

1. Introduction

Radio galaxies display a wide range of structures in radio images. The most common large-scale structures are called lobes: these are double, often fairly symmetrical, roughly ellipsoidal structures placed on either side of the active nucleus. A significant minority of low-luminosity sources exhibit structures usually known as plumes which are much more elongated. Some radio galaxies show one or two long narrow features known as jets coming directly from the nucleus and going to the lobes. Hence, the radio galaxies morphologically are divided into FR I and FR II types. The FR I objects ('edge-darkened doubles') generally contain prominent, often two-sided jets, with the lobe emission trailing off into intergalactic space. Whereas, the FR II objects ('edge-brightened doubles', 'classical doubles') contain hot spots in one or both lobes.

It seems that FR II radio galaxies (see Fig. 1) are usually isolated field sources and form a remarkably homogeneous set. On the other hand, the FR I radio galaxies are much more varied. They are not only found as isolated field sources, they are also often found in clusters (Perley 1989). For example, head-tail galaxies, which are FR I objects, are almost always associated with clusters of galaxies and are characterized by a highly elongated radio structure with the associated optical galaxy at one end. A classical example (see Fig. 2) is 3C 129 (a narrow-angle-tail) which, along with its companion 3C 129.1 (a wide-angle-tail), is a member of an X-ray cluster. In the canonical picture, the characteristic shape is explained by the kinematics of the source, which is governed by the dominant gravitational force in the cluster and the properties of the beams and jets (Lal & Rao 2004). Similarly, wide-angle-tail galaxies are intermediate between standard FR I and FR II objects, with collimated jets and sometimes hotspots, but with plumes rather than lobes, found at or near the centres of clusters. Here again, the characteristic shape is mainly due to the dominant gravitational force in the cluster.

Therefore, the general morphology of radio sources lends encouragement to ideas of confinement, or at least radio morphology partly governed by an external gas (Hardcastle 2005, and see Hardcastle in this proceeding), but some objects persist in complicating the simple picture. For example, B1059+169 (Fig. 3) which shows X-shaped structure. Such sources are characterized by two axes, the ‘wing’ axis oriented at an angle to the ‘active’ axis, giving the total source an ‘X’ shape. These two sets of lobes usually pass symmetrically through the centre of the associated host galaxy, and the majority of these sources are FR II and the rest are either FR I or mixed. These have been modelled via backflow from the lobes along with buoyancy-driven outflow. Precession of the radio axis also comes to mind. They have also been put forth as derivatives of central engines that have been reoriented, perhaps due to a minor merger. Alternatively, they may also result from two pairs of jets that are associated with a pair of unresolved AGNs (see Lal & Rao 2007 for a detailed summary). The key point is that interpretation of radio source morphology, in general, is not necessarily simple.

Spectral ageing Under the standard model of a FR II source evolution, the source grows longer as the jet pushes back the external medium. If there is no significant re-acceleration within the lobes and no significant transport of particles since the last acceleration, then the central regions are ‘older’ than the outer regions, in the sense that particles located in the central regions were processed through the hot spot shock at a time before those currently radiating at the ends of the radio source. Hence, the spectral index of the radiation from the central regions should have a steeper spectral index than that at the ends. Whereas, in the case of FR I sources, e.g., in almost all head-tail and wide-angle-tail galaxies, the radio spectrum has been found to steepen with distance along the tail and has been interpreted in terms of ageing of electron population.

Finally, in several of the formation scenarios mentioned above for X-shaped sources, the wings are interpreted as relics of past radio jets and the active lobes as the newer ones. Hence, the wings are expected to show steeper spectra than the active lobes in standard models for electron energy evolution.

2. Observations and Data Analysis

In recent years we have used the GMRT (Rao 2002) to study morphology of several radio galaxies at 240 MHz and 610 MHz, with a resolution of about 10 arcsec and 5 arcsec, respectively. The GMRT visibility data were analyzed using `APRS` in the standard manner. All details of the analysis procedures used are given in Lal et al. (2008).

The GMRT has a hybrid configuration with 14 of its 30 antennae located in a central compact array with a size 1.1 km (comparable to the VLA D configuration) and the remaining antennae distributed in a roughly ‘Y’-shaped configuration, giving a maximum baseline length of 25 km (comparable to the VLA B configuration). Hence, a single observation with the GMRT samples the (u, v) plane on both short and long baselines, and can map detailed source structure with a reasonably good sensitivity.

3. Results

I bring together two remarkable results obtained using GMRT.

Similar/Dis-similar radio morphologies It is remarkably unusual that any FR II source has a morphology at low radio frequency (less than a few hundred MHz) that is different

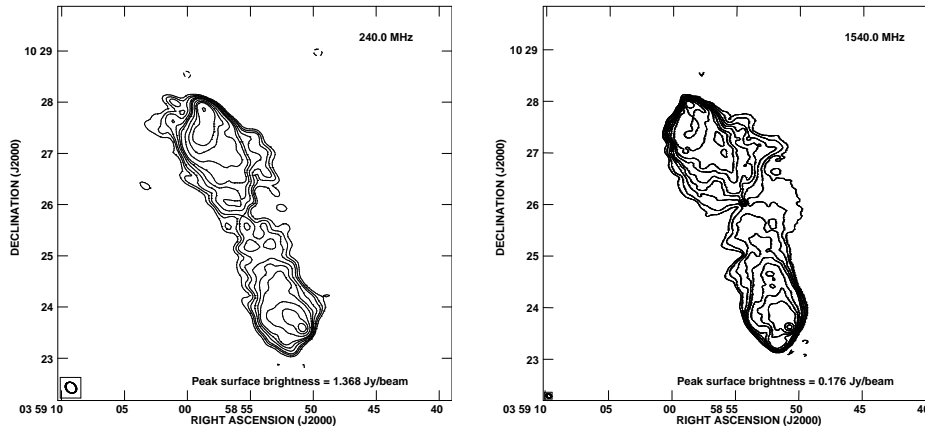


Figure 1. GMRT map of 3C 98 at 240 MHz (left panel) and the 1.5 GHz map (right panel) from the Atlas catalog. (Available at <http://www.jb.man.ac.uk/atlas/~>.)

from its high radio frequency (GHz) morphology. Fig. 1 shows 3C 98 as an example showing similar radio morphologies at 240 MHz and 1.5 GHz. In addition the 74 MHz and the 4.9 GHz radio morphologies are also identical. The observations of some 3C radio galaxies at 151 MHz and 1.4 GHz (Leahy et al. 1989) show that the lobe lengths at these different frequencies are the same and they also suggest that the particles responsible for the low-frequency emission are entirely co-spatial with those responsible for the high-frequency emission. This suggests that synchrotron-emitting particles of all energies permeate the lobe magnetic field in the same way, despite the fact that the higher energy particles have shorter radiative lifetimes than the lower energy ones. This hints that low-frequency synchrotron emission fades (nearly) as rapidly as high-frequency synchrotron emission (Blundell 2008); and so, are the observations really inconsistent with the idea that synchrotron cooling is not the dominant energy-loss mechanism for the synchrotron plasma? Hardcastle & Looney (2008) note that by the time we get to 100 GHz there really are fairly obvious morphological differences in lobes, although the sensitivity of those observations is not great. Whereas, the FR I sources, in particular the head-tail galaxies and wide-angle-tail galaxies show signs of synchrotron cooling in spectral index images (Lal & Rao 2004) made using narrow frequency spacing (240 MHz and 1.4 GHz) and often show the presence of steep spectrum diffuse emission at low radio frequencies, which is not seen at high radio frequencies (Fig. 2).

Nevertheless, in the light of above data, our results provide evidence that there exists two class of sources linked to FR I/FR II sources on morphological grounds. In one, where the low frequency radio images show morphologies that are dis-similar to the morphologies at high frequencies, consistent with the simple picture of spectral electron ageing. In the other, where the low frequency radio images show morphologies that are similar to the morphologies at high frequencies, which, possibly, suggests that the simple picture of spectral ageing needs revision. In more detail, it seems that along with the simple FR I/FR II division, which depends on host-galaxy environment in the sense that the FR I/FR II transition appears at higher luminosities in more massive galaxies, the role played by the intracluster gas in deciding the source morphology is also important. In particular, the role of dominant gravitational force in the clus-

ter in defining the source morphology cannot be ignored, which possibly is key to the physical origin of the above two classes of sources.

Low surface brightness features having flat spectra Fig. 3 shows B1059+169, a X-shaped radio source seen in a cluster environment (Abell 1145), which is the dominant radio galaxy and is 5.5 arcmin away from the cluster centre. A companion is detected on the 2MASS, coincident with the cluster centre. Although the source is found in the cluster environment, surprisingly, its spectral index map is unusual, that is, the wings have relatively flatter spectral index compared to the active lobes. Therefore, we remark that whenever there is a low-surface brightness feature attached to a radio galaxy, it is not necessary that it should be a steep spectrum feature.

In addition, if our understanding of synchrotron spectral ageing at low radio frequencies is correct, then the spectral index results do not favour several of the formation models for the X-shaped sources. One plausible model is the Lal & Rao (2005, 2007) model in which X-shaped sources consist of two pairs of jets, which are associated with two unresolved AGN. However, exceptions exist, e.g., in the case of 3C 403, Kraft et al. (2005) favoured the hydrodynamic model.

4. Looking Ahead

Presently the GMRT observations have provided several high resolution, high sensitivity images, and it is now possible to probe, statistically, the morphological properties of radio sources. I have presented above two unusual results, but it will still be important to obtain observations using GMRT of complete, unbiased samples of radio galaxies to draw general conclusions about the population of radio galaxies as a whole.

Acknowledgments. We thank the staff of the GMRT that made these observations possible. GMRT is run by the NCRA of the TIFR. I warmly thank my collaborators M.J. Hardcastle, R.P. Kraft and A.P. Rao and especially A.L. Roy for a careful reading of this manuscript.

References

- Blundell, K.M. 2008, in *Extragalactic Jets: Theory and Observation from Radio to Gamma Ray*, ed. Travis A. Rector & David S. De Young (San Francisco: ASP) 386, p. 467
 Hardcastle, M.J., & Looney, L.W. 2008, *MNRAS*, 388, 176
 Hardcastle, M.J. 2005, *Phil. Trans. R. Soc. A*, 363, 2711
 Kraft, R.P., Hardcastle, M.J., Worrall, D.M., & Murray, S.S. 2005, *ApJ*, 622, 149
 Lal, D.V., Hardcastle, M.J., & Kraft, R.P. 2008, *MNRAS*, 390, 1105
 Lal, D.V., & Rao, A.P. 2007, *MNRAS*, 374, 1085
 Lal, D.V., & Rao, A.P. 2005, *MNRAS*, 356, 232
 Lal, D.V., & Rao, A.P. 2004, *A&A*, 420, 491
 Leahy, J.P., Muxlow, T.W.B., & Stephens, P.W. 1989, *MNRAS*, 239, 401
 Perley, R.A. 1989, in *Proceedings of a Workshop Held at Ringberg Castle, Lecture Notes in Physics* (Springer Berlin / Heidelberg), 327, 1
 Rao, A.P. 2002, in *IAU Symposium 199, The Universe at Low Radio Frequencies*, ed. A.P. Rao, G. Swarup & Gopal-Krishna (San Francisco: ASP), p. 439

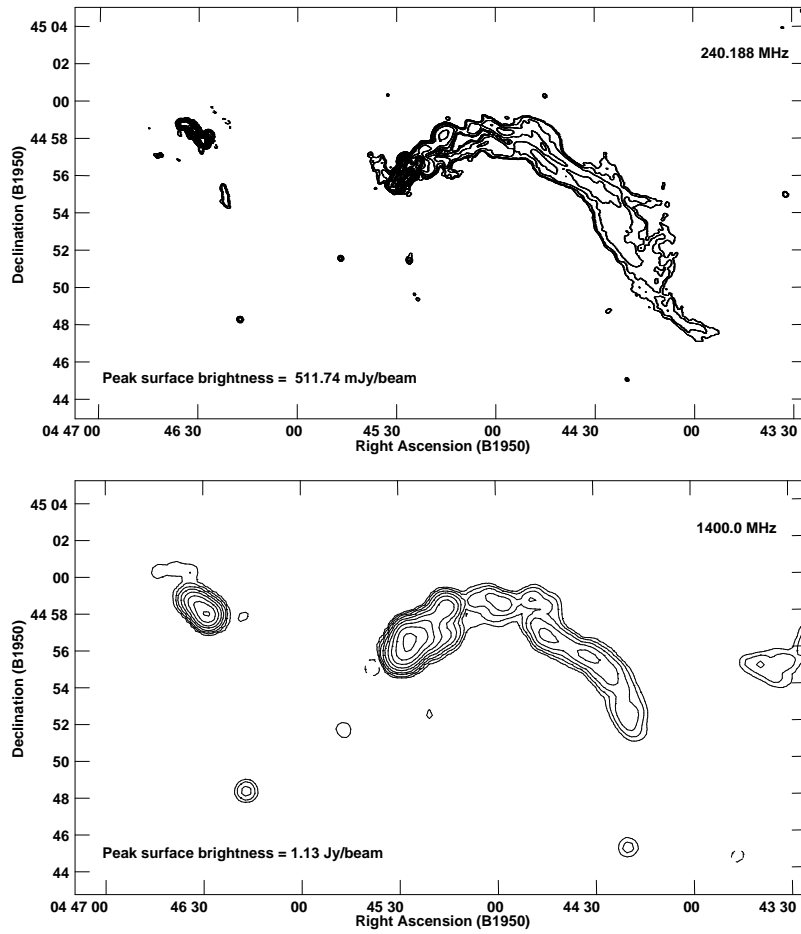


Figure 2. Full synthesis GMRT map of 3C 129 at 240 MHz (upper panel) showing larger projected angular size than the NVSS map at 1.4 GHz (lower panel).

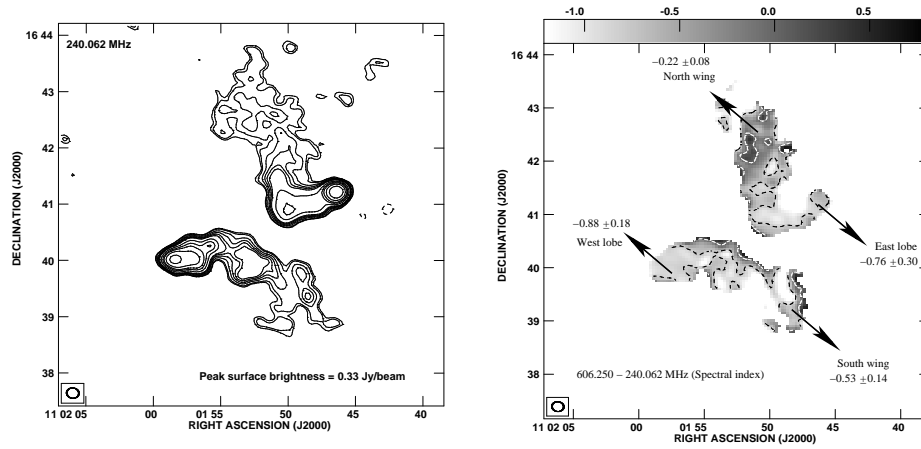


Figure 3. GMRT map of B1059+169 at 240 MHz (left panel) and the distribution of the spectral index between 240 MHz and 610 MHz (right panel), where $S_\nu \propto \nu^\alpha$.